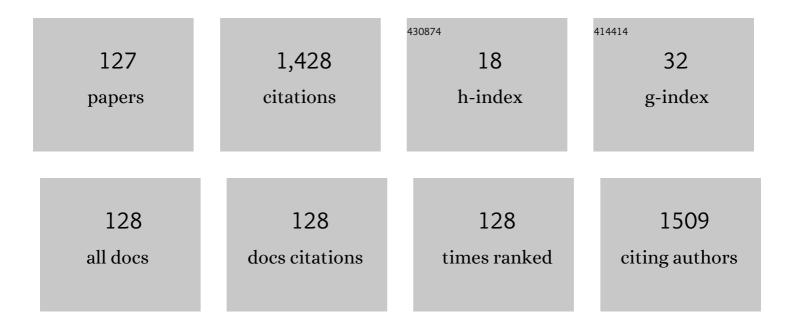
## Ahmad Mohd Khairul

List of Publications by Year in descending order

Source: https://exaly.com/author-pdf/1598396/publications.pdf Version: 2024-02-01



#	Article	IF	CITATIONS
1	Electrochemical-Based Biosensors on Different Zinc Oxide Nanostructures: A Review. Materials, 2019, 12, 2985.	2.9	108
2	Surface Study of CuO Nanopetals by Advanced Nanocharacterization Techniques with Enhanced Optical and Catalytic Properties. Nanomaterials, 2020, 10, 1298.	4.1	98
3	Cytotoxicity of MXene-based nanomaterials for biomedical applications: A mini review. Environmental Research, 2021, 201, 111592.	7.5	91
4	Fabrication of hierarchical Sn-doped ZnO nanorod arrays through sonicated solâ^'gel immersion for room temperature, resistive-type humidity sensor applications. Ceramics International, 2016, 42, 9785-9795.	4.8	68
5	Synthesis, characterization and antifungal property of Ti3C2Tx MXene nanosheets. Ceramics International, 2020, 46, 20306-20312.	4.8	55
6	Industrial textile wastewater treatment via membrane photocatalytic reactor (MPR) in the presence of ZnO-PEG nanoparticles and tight ultrafiltration. Journal of Water Process Engineering, 2019, 31, 100872.	5.6	48
7	Synthesis, structural and optical properties of mesostructured, X-doped NiO (x = Zn, Sn, Fe) nanoflake network films. Materials Research Bulletin, 2020, 127, 110860.	5.2	45
8	A comparative study of ZnO-PVP and ZnO-PEG nanoparticles activity in membrane photocatalytic reactor (MPR) for industrial dye wastewater treatment under different membranes. Journal of Environmental Chemical Engineering, 2019, 7, 103143.	6.7	35
9	Controlled Growth of Zinc Oxide Nanorods by Aqueous-Solution Method. Synthesis and Reactivity in Inorganic, Metal Organic, and Nano Metal Chemistry, 2010, 40, 190-194.	0.6	29
10	Effect of oxygen flow rate on the ultraviolet sensing properties of zinc oxide nanocolumn arrays grown by radio frequency magnetron sputtering. Ceramics International, 2016, 42, 4107-4119.	4.8	29
11	Growth of titanium dioxide nanorod arrays through the aqueous chemical route under a novel and facile low-cost method. Materials Letters, 2016, 164, 294-298.	2.6	29
12	Enhanced humidity sensing performance using Sn-Doped ZnO nanorod Array/SnO2 nanowire heteronetwork fabricated via two-step solution immersion. Materials Letters, 2018, 210, 258-262.	2.6	29
13	Raman investigation of rutile-phased TiO2 nanorods/nanoflowers with various reaction times using one step hydrothermal method. Journal of Materials Science: Materials in Electronics, 2016, 27, 7920-7926.	2.2	28
14	Dye-sensitized solar Cell using pure anatase TiO2 annealed at different temperatures. Optik, 2017, 140, 1063-1068.	2.9	28
15	Alginate-gelatin bioink for bioprinting of hela spheroids in alginate-gelatin hexagon shaped scaffolds. Polymer Bulletin, 2021, 78, 6115-6135.	3.3	26
16	Improving the photovoltaic performance of DSSCs using a combination of mixed-phase TiO2 nanostructure photoanode and agglomerated free reduced graphene oxide counter electrode assisted with hyperbranched surfactant. Optik, 2018, 158, 522-534.	2.9	25
17	Enhanced photovoltaic performance using reduced graphene oxide assisted by triple-tail surfactant as an efficient and low-cost counter electrode for dye-sensitized solar cells. Optik, 2017, 139, 291-298.	2.9	21
18	Fabrication and characterization of rutile-phased titanium dioxide (TiO2) nanorods array with various reaction times using one step hydrothermal method. Optik, 2018, 154, 510-515.	2.9	20

#	Article	IF	CITATIONS
19	Incorporation of Electrochemically Exfoliated Graphene Oxide and TiO2 into Polyvinylidene Fluoride-Based Nanofiltration Membrane for Dye Rejection. Water, Air, and Soil Pollution, 2019, 230, 1.	2.4	20
20	Electrical enhancement of radiation-vulcanized natural rubber latex added with reduced graphene oxide additives for supercapacitor electrodes. Journal of Materials Science, 2017, 52, 6611-6622.	3.7	19
21	Synthesis, transfer and application of graphene as a transparent conductive film: a review. Bulletin of Materials Science, 2020, 43, 1.	1.7	18
22	Reduced graphene oxide-multiwalled carbon nanotubes hybrid film with low Pt loading as counter electrode for improved photovoltaic performance of dye-sensitised solar cells. Journal of Materials Science: Materials in Electronics, 2018, 29, 10723-10743.	2.2	17
23	Modulation of Sn concentration in ZnO nanorod array: intensification on the conductivity and humidity sensing properties. Journal of Materials Science: Materials in Electronics, 2018, 29, 12076-12088.	2.2	17
24	Enhancing the performance of self-powered ultraviolet photosensor using rapid aqueous chemical-grown aluminum-doped titanium oxide nanorod arrays as electron transport layer. Thin Solid Films, 2018, 655, 1-12.	1.8	16
25	Photocatalytic degradation of methylene blue by flowerlike rutile-phase TiO2 film grown via hydrothermal method. Journal of Sol-Gel Science and Technology, 2022, 102, 637-648.	2.4	16
26	Enhanced field electron emission of flower-like zinc oxide on zinc oxide nanorods grown on carbon nanotubes. Materials Letters, 2015, 149, 66-69.	2.6	15
27	Hydrothermal growth of bilayered rutile-phased TiO2 nanorods/micro-size TiO2 flower in highly acidic solution for dye-sensitized solar cell. Journal of Sol-Gel Science and Technology, 2015, 73, 655-659.	2.4	15
28	Preparation of conductive cellulose paper through electrochemical exfoliation of graphite: The role of anionic surfactant ionic liquids as exfoliating and stabilizing agents. Carbohydrate Polymers, 2018, 201, 48-59.	10.2	15
29	Optimization of a Hydrothermal Growth Process for Low Resistance 1D Fluorine-Doped Zinc Oxide Nanostructures. Journal of Nanomaterials, 2019, 2019, 1-10.	2.7	15
30	Influence of TiO2 layer's nanostructure on its thermoelectric power factor. Applied Surface Science, 2019, 497, 143736.	6.1	15
31	Direct and seedless growth of Nickel Oxide nanosheet architectures on ITO using a novel solution immersion method. Materials Letters, 2019, 236, 460-464.	2.6	15
32	Surfactants with aromatic headgroups for optimizing properties of graphene/natural rubber latex composites (NRL): Surfactants with aromatic amine polar heads. Journal of Colloid and Interface Science, 2019, 545, 184-194.	9.4	14
33	Interface study of hybrid CuO nanoparticles embedded ZnO nanowires heterojunction synthesized by controlled vapor deposition approach for optoelectronic devices. Optical Materials, 2021, 117, 111132.	3.6	14
34	Review—Three Dimensional Zinc Oxide Nanostructures as an Active Site Platform for Biosensor: Recent Trend in Healthcare Diagnosis. Journal of the Electrochemical Society, 2020, 167, 137501.	2.9	14
35	Scaled-up prototype of carbon nanotube production system utilizing waste cooking palm oil precursor and its nanocomposite application as supercapacitor electrodes. Journal of Materials Science: Materials in Electronics, 2016, 27, 11599-11605.	2.2	13
36	Fabrication, structural, optical, electrical, and humidity sensing characteristics of hierarchical NiO nanosheet/nanoball-flower-like structure films. Journal of Materials Science: Materials in Electronics, 2020, 31, 11673-11687.	2.2	13

#	Article	IF	CITATIONS
37	Performance of membrane photocatalytic reactor incorporated with ZnO-Cymbopogon citratus in treating palm oil mill secondary effluent. Chemical Engineering Research and Design, 2020, 143, 273-284.	5.6	13
38	Photocatalytic performance improvement by utilizing GO_MWCNTs hybrid solution on sand/ZnO/TiO2-based photocatalysts to degrade methylene blue dye. Environmental Science and Pollution Research, 2021, 28, 6966-6979.	5.3	13
39	Synthesis and field electron emission properties of waste cooking palm oil-based carbon nanotubes coated on different zinc oxide nanostructures. Journal of Alloys and Compounds, 2016, 656, 368-377.	5.5	12
40	Elucidation of synergistic effect of eucalyptus globulus honey and Zingiber officinale in the synthesis of colloidal biogenic gold nanoparticles with antioxidant and catalytic properties. Sustainable Chemistry and Pharmacy, 2019, 13, 100156.	3.3	12
41	Hierarchically assembled tin-doped zinc oxide nanorods using low-temperature immersion route for low temperature ethanol sensing. Journal of Materials Science: Materials in Electronics, 2017, 28, 16292-16305.	2.2	11
42	Hydrothermal synthesis of biocompatible nitrogen doped graphene quantum dots. Energy and Environment, 2021, 32, 1170-1182.	4.6	11
43	Electrochemical exfoliation of graphite in nanofibrillated kenaf cellulose (NFC)/surfactant mixture for the development of conductive paper. Carbohydrate Polymers, 2020, 228, 115376.	10.2	10
44	ZnO nanowires based schottky contacts of Rh/ZnO interfaces for the enhanced performance of electronic devices. Surfaces and Interfaces, 2020, 21, 100649.	3.0	10
45	Surface chemistry and growth mechanism of highly oriented, single crystalline Nb-doped TiO <sub>2</sub> nanorods. CrystEngComm, 2020, 22, 2380-2388.	2.6	10
46	Effect of heat treatment to the rutile based dye sensitized solar cell. Optik, 2016, 127, 4076-4079.	2.9	9
47	Hydrophobic rutile phase TiO2 nanostructure and its properties for self-cleaning application. AIP Conference Proceedings, 2017, , .	0.4	9
48	Low-temperature-dependent growth of titanium dioxide nanorod arrays in an improved aqueous chemical growth method for photoelectrochemical ultraviolet sensing. Journal of Materials Science: Materials in Electronics, 2019, 30, 1017-1033.	2.2	9
49	Effect of Surfactants' Tail Number on the PVDF/GO/TiO2-Based Nanofiltration Membrane for Dye Rejection and Antifouling Performance Improvement. International Journal of Environmental Research, 2021, 15, 149-161.	2.3	9
50	Carbon nanotubes from waste cooking palm oil as adsorbent materials for the adsorption of heavy metal ions. Environmental Science and Pollution Research, 2021, 28, 65171-65187.	5.3	9
51	Performance comparison between silicon solar panel and dye-sensitized solar panel in Malaysia. AIP Conference Proceedings, 2017, , .	0.4	8
52	Structural, optical, and electrical evolution of sol–gel-immersion grown nickel oxide nanosheet array films on aluminium doping. Journal of Materials Science: Materials in Electronics, 2019, 30, 9916-9930.	2.2	8
53	Improved DSSC photovoltaic performance using reduced graphene oxide–carbon nanotube/platinum assisted with customised triple-tail surfactant as counter electrode and zinc oxide nanowire/titanium dioxide nanoparticle bilayer nanocomposite as photoanode. Graphene Technology, 2019. 4. 17-31.	1.9	8
54	Highly branched triple-chain surfactant-mediated electrochemical exfoliation of graphite to obtain graphene oxide: colloidal behaviour and application in water treatment. Physical Chemistry Chemical Physics, 2020, 22, 12732-12744.	2.8	8

Ahmad Mohd Khairul

#	Article	IF	CITATIONS
55	Sputter Deposition of Cuprous and Cupric Oxide Thin Films Monitored by Optical Emission Spectroscopy for Gas Sensing Applications. Procedia Chemistry, 2016, 20, 124-129.	0.7	7
56	Electrical Properties and Surface Morphology Study on the Effect of Annealing Temperature of One Layer Titanium Dioxide Thin Films Prepared by Sol-Gel Method. , 2009, , .		6
57	Amorphous Al–Cu alloy nanowires decorated with carbon spheres synthesised from waste engine oil. Journal of Alloys and Compounds, 2015, 642, 111-116.	5.5	6
58	A scaffoldless technique for self-generation of three-dimensional keratinospheroids on liquid crystal surfaces. Biotechnic and Histochemistry, 2016, 91, 283-295.	1.3	6
59	Correlation between Microstructure of Copper Oxide Thin Films and its Gas Sensing Performance at Room Temperature. Procedia Chemistry, 2016, 20, 45-51.	0.7	6
60	Physical and rheological properties of Titanium Dioxide modified asphalt. E3S Web of Conferences, 2018, 34, 01035.	0.5	6
61	Advanced Nanoscale Surface Characterization of CuO Nanoflowers for Significant Enhancement of Catalytic Properties. Molecules, 2021, 26, 2700.	3.8	6
62	Effect of Annealing Temperature on Titanium Dioxide Thin Films Prepared by Sol Gel Method. AIP Conference Proceedings, 2008, , .	0.4	5
63	Influence of Glacial Acetic Acid and Nitric Acid as a Chelating Agent in Sol-gel Process to the Nanostructured Titanium Dioxide Thin Films. , 2009, , .		5
64	Influence of outlet channel width to the flow velocity and pressure of a flow focusing microfluidic device. IOP Conference Series: Materials Science and Engineering, 2016, 160, 012086.	0.6	5
65	Zero voltage switching driver and flyback transformer for generation of atmospheric pressure plasma jet. AIP Conference Proceedings, 2017, , .	0.4	5
66	Atmospheric pressure plasma needle jet treated on aluminium thin film for semiconductor industries. Materials Today: Proceedings, 2019, 7, 715-720.	1.8	5
67	Adsorption effect of oxygen on ZnO Nanowires (100 nm) leading towards pronounced edge effects and voltage enhancement. Materials Research Express, 2020, 7, 095004.	1.6	5
68	The potential control strategies of membrane fouling and performance in membrane photocatalytic reactor (MPR) for treating palm oil mill secondary effluent (POMSE). Chemical Engineering Research and Design, 2020, 162, 12-27.	5.6	4
69	The utilization of waste cooking palm oil as a green carbon source for the growth of multilayer graphene. Journal of the Australian Ceramic Society, 2021, 57, 347-358.	1.9	4
70	Fabrication and application of composite adsorbents made by one-pot electrochemical exfoliation of graphite in surfactant ionic liquid/nanocellulose mixtures. Physical Chemistry Chemical Physics, 2021, 23, 19313-19328.	2.8	4
71	Enhancement of spin Seebeck effect of reverse spin crossover Fe (II) micellar charge transport using PMMA polymer electrolyte. Applied Organometallic Chemistry, 2021, 35, e6268.	3.5	4
72	Influence of annealing temperature on the sensitivity of nickel oxide nanosheet films in humidity sensing applications. Indonesian Journal of Electrical Engineering and Computer Science, 2020, 18, 284.	0.8	4

Ahmad Mohd Khairul

#	Article	IF	CITATIONS
73	Effect of anneal temperature on fluorine doped tin oxide (FTO) nanostructured fabricated using hydrothermal method. AIP Conference Proceedings, 2017, , .	0.4	3
74	Comparison of biophysical properties characterized for microtissues cultured using microencapsulation and liquid crystal based 3D cell culture techniques. Cytotechnology, 2018, 70, 13-29.	1.6	3
75	Physical and rheological properties of nano zinc oxide modified asphalt binder. MATEC Web of Conferences, 2018, 250, 02004.	0.2	3
76	Effect of post annealing treatment on electrical and structural properties of zinc oxide nanostructures. Materials Today: Proceedings, 2019, 7, 710-714.	1.8	3
77	Adsorption effect of NO2 on ZnO (100 nm) nanowires, leading towards reduced reverse leakage current and voltage enhancement. Bulletin of Materials Science, 2020, 43, 1.	1.7	3
78	Effects of TiO2 phase and nanostructures as photoanode on the performance of dye-sensitized solar cells. Bulletin of Materials Science, 2021, 44, 1.	1.7	3
79	Significant effect of concentration ratio in synthesizing titania nanoflowers (TNF) powder for various application as additive. Malaysian Journal of Fundamental and Applied Sciences, 2018, 14, 397-402.	0.8	3
80	Highly Porous NiO Nanoflower-based Humidity Sensor Grown on Seedless Glass Substrate via One-Step Simplistic Immersion Method. International Journal of Engineering and Advanced Technology, 2019, 9, 5718-5722.	0.3	3
81	Study of cobalt doping on the electrical and optical properties of titanium dioxide thin film prepared by sol-gel method. , 2008, , .		2
82	Morphology, topography and thickness of copper oxide thin films deposited using magnetron sputtering technique. , 2013, , .		2
83	Electrical and Structural Properties of TiO <sub>2 </sub> Thin Film Prepared at Different Annealing Temperatures by Sol-Gel Spin-Coating Method. Advanced Materials Research, 2013, 667, 371-374.	0.3	2
84	Development of atmospheric pressure plasma needle jet for sterilization applications. AIP Conference Proceedings, 2017, , .	0.4	2
85	Fabrication of TiO2 nanostructures on porous silicon for thermoelectric application. AIP Conference Proceedings, 2017, , .	0.4	2
86	Rutile Phased Titanium Dioxide (TiO2) Nanorod/Nanoflower Based Waste Water Treatment Device. Advances in Intelligent Systems and Computing, 2017, , 483-490.	0.6	2
87	Improvement in photo voltaic performance of rutile-phased TiO2 nanorod/nanoflower-based dye-sensitized solar cell. Journal of the Australian Ceramic Society, 2018, 54, 663-670.	1.9	2
88	Plasma diagnostic by optical emission spectroscopy on reactive magnetron sputtering plasma –A Brief Introduction. Journal of Physics: Conference Series, 2018, 1027, 012005.	0.4	2
89	Seebeck coefficient of synthesized Titanium Dioxide thin film on FTO glass substrate. IOP Conference Series: Materials Science and Engineering, 2018, 342, 012051.	0.6	2
90	High responsivity of ultraviolet sensor-based rutile-phased TiO2 nanorod arrays using different bias voltage. Journal of the Australian Ceramic Society, 2020, 56, 461-468.	1.9	2

#	Article	IF	CITATIONS
91	Influence of Doping Concentration on the Zinc Doped Nickel Oxide Nanostructures: Morphological, Structural, and Optical Properties. IOP Conference Series: Earth and Environmental Science, 2021, 682, 012070.	0.3	2
92	The investigation of chlorpyrifos (Cpy) detection of PEDOT:PSS-MXene(Ti2CTX)-BSA-GO composite using P-ISFET reduction method. Polymer Bulletin, 2023, 80, 1243-1264.	3.3	2
93	A guide to designing graphene-philic surfactants. Journal of Colloid and Interface Science, 2022, 620, 346-355.	9.4	2
94	Effect of anatase TiO <inf>2</inf> overlayer on the photovoltaic properties of rutile phase nanostructured dye-sensitized solar cell. , 2013, , .		1
95	Effect of Substrate Bias in Copper Sputtering Plasma Measured by Langmuir Probe. Advanced Materials Research, 0, 925, 238-242.	0.3	1
96	Electrical and optical characteristics of atmospheric pressure plasma needle jet driven by neon trasformer. AIP Conference Proceedings, 2017, , .	0.4	1
97	Development of a Microfluidic Device System Using Adhesive Vinyl Template to Produce Calcium Alginate Microbeads for Microencapsulation of Cells. Advances in Intelligent Systems and Computing, 2017, , 477-482.	0.6	1
98	Effect of working power and pressure on plasma properties during the deposition of TiN films in reactive magnetron sputtering plasma measured using Langmuir probe measurement. Journal of Physics: Conference Series, 2018, 995, 012068.	0.4	1
99	Fabrication of Nanorods-TiO2 for Heterojunction Thin Film Application with Electrodeposit-p-Cu2O Absorbing Layer. Materials Today: Proceedings, 2019, 18, 468-472.	1.8	1
100	Generation of HeLa spheroids in Ca-alginate-PEG microbeads using flicking technique as an improved three-dimensional cell culture system. Colloids and Surfaces A: Physicochemical and Engineering Aspects, 2020, 599, 124885.	4.7	1
101	INFLUENCES OF DEPOSITION TIME ON TIO2 THIN FILMS PROPERTIES PREPARED BY CVD TECHNIQUE. Jurnal Teknologi (Sciences and Engineering), 2016, 78, .	0.4	1
102	3D Oral Squamous Cell Carcinoma Microtissues Grown in Calcium Alginate Microbeads. Annual Research & Review in Biology, 2017, 13, 1-12.	0.4	1
103	Comparison of Deposition Methods of ZnO Thin Film on Flexible Substrate. Indonesian Journal of Electrical Engineering and Computer Science, 2017, 5, 536.	0.8	1
104	Photovoltaic enhancement of nanostructured boron-doped rutile phase TiO2 nanorods via facile hydrothermal method. Journal of Materials Science: Materials in Electronics, 0, , 1.	2.2	1
105	Study on the Effect of Different Amount of Titanium Dioxide Nano-Powder to the Nano-Structured Titanium Dioxide Thin Films. , 2009, , .		0
106	Surface Morphology and Optical Property Studies of Nanostructured Titanium Dioxide. , 2009, , .		0
107	Study on the Ohmic Contact, Electrical and Optical Properties of Nanostructured Titanium Dioxide Thin Films. , 2009, , .		0
108	Study on the Effect of Various Sol-Gel Concentration to the Electrical, Structural and Optical Properties of the Nanostructured Titanium Dioxide Thin Films. , 2009, , .		0

#	Article	IF	CITATIONS
109	The Study of Physical Properties on Nanostructured Titanium Dioxide Thin Film Annealed at Different Temperatures. , 2009, , .		0
110	Structural characterization of zinc oxide thin films deposited at various O <inf>2</inf> /Ar flow ratio in magnetron sputtering plasma. , 2013, , .		0
111	Influence of Dissipation Power in Copper Sputtering Plasma Measured by Optical Emission Spectroscopy. Advanced Materials Research, 2013, 832, 243-247.	0.3	0
112	Numerical estimation of self-sputtering effect in ionized physical vapor deposition system. , 2014, , .		0
113	Correlation between the microstructure of copper oxide thin film and its gas sensing response. , 2014, , .		0
114	Hardware and circuit design of a vibrational cleaner. IOP Conference Series: Materials Science and Engineering, 2016, 160, 012085.	0.6	0
115	THE PHYSICAL AND RHEOLOGICAL CHARACTERISTICS OF MODIFIED ASPHALT BINDER WITH TITANIUM DIOXIDE R15. Jurnal Teknologi (Sciences and Engineering), 2016, 78, .	0.4	0
116	Characterisation of encapsulated cells in calcium alginate microcapsules. , 2016, , .		0
117	Hydrophilic property of glass treated by needle plasma jet for surface modification. , 2016, , .		0
118	Growth of microtissues in microencapsules formed using microextrusion and vibration. , 2016, , .		0
119	Comparative study between chemical and atmospheric pressure plasma jet cleaning on glass substrate. AIP Conference Proceedings, 2017, , .	0.4	0
120	Atmospheric pressure plasma jet's characterization and surface wettability driven by neon transformer. AIP Conference Proceedings, 2017, , .	0.4	0
121	The piezoelectric effect on zinc oxide nano on polyimide substrate by spray pyrolysis. AIP Conference Proceedings, 2017, , .	0.4	0
122	Nitrogen emission in reactive magnetron sputtering plasmas during the deposition of titanium nitride thin film. AIP Conference Proceedings, 2017, , .	0.4	0
123	Laboratory Study on the Fatigue Resistance of Asphaltic Concrete Containing Titanium Dioxide. E3S Web of Conferences, 2018, 34, 01021.	0.5	0
124	Development of a Microdilution Device with One-step Dilution of Cytochalasin-B for Treating ORL-48 Cancer Microtissues. Biotechnology and Bioprocess Engineering, 2019, 24, 761-772.	2.6	0
125	Characterization of Amorphous GaN Thin Films after Conventional Thermal Anneal. , 2020, , .		0
126	Optimum Reduced Graphene Oxide (rGO) Volume for Hydrothermal Synthesis of Titanium Dioxide (TiO2) Nanostructure Direct Growth on Fluorine-Doped Tin Oxide (FTO)/rGO Substrate. Journal of Computational and Theoretical Nanoscience, 2020, 17, 886-892.	0.4	0

#	Article	IF	CITATIONS
127	Structural and photoluminescence properties of Zinc oxide nanowires synthesized by smart thermal CVD method. , 2021, , .		0